

AD-A161 814

AVERAGE COLLISIONAL VIBRATIONAL ENERGY TRANSFER
QUANTITIES THE EXPONENTIAL (U) WASHINGTON UNIV SEATTLE
DEPT OF CHEMISTRY B S RABINOVITCH 15 NOV 85

1/1

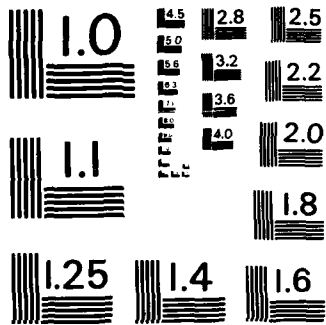
UNCLASSIFIED

NR092-549-TR32 N00014-75-C-0690

F/G 20/0

NL

								END					
								FILED					
								DTIC					



MICROCOPY RESOLUTION TEST CHART
NATIONAL BUREAU OF STANDARDS-1963-A

12

Average Collisional Vibrational Energy Transfer
Quantities. The Exponential Model

B. S. Rabinovitch

Department of Chemistry BG-10
University of Washington
Seattle, Washington 98195

Technical Report No. NR092-549-TR32
Contract N00014-75-C-0690, NR-092-549

November 15, 1985

Prepared for Publication in J. Phys. Chem.

AD-A161 814

DTIC FILE COPY

OFFICE OF NAVAL RESEARCH
Department of the Navy, Code 432
800 N. Quincy
Arlington, VA 22217

DTIC
EXECTE
NOV 26 1985
S D

85. 11 22 024

Reproduction in whole or in part is permitted for any purpose of the United States Government. This document has been approved for public release; its distribution is unlimited.

AVERAGE COLLISIONAL VIBRATIONAL ENERGY TRANSFER QUANTITIES.

THE EXPONENTIAL MODEL

D. C. Tardy

Department of Chemistry, University of Iowa, Iowa City, Iowa 52242

and

B. S. Rabinovitch

Department of Chemistry, University of Washington, Seattle, Washington 98195

Abstract

The important collisional energy transfer ratio, $\gamma = \langle \Delta E \rangle_{\text{all}} / \langle \Delta E \rangle_d$ was examined by using a fitted classical approximation for the density of internal energy eigenstates. The exponential form of the collisional energy transfer probability function was applied to four model unimolecular reaction systems. Two parameters, the inversion temperature T_I and the effective temperature T_e (defined previously in I), were employed to develop a form for the parametric dependence of γ on $\langle \Delta E \rangle_d$, energy level E and temperature T ; these quantities are related to a reduced average energy transfer quantity E'_d . Comparison was made with previous literature expressions for the inter-relationship between $\langle \Delta E \rangle_{\text{all}}$ and $\langle \Delta E \rangle_d$ for both exponential and stepladder models of the collisional transition probabilities. For small E'_d , $\langle \Delta E \rangle_d^{\text{EXP}} = 0.7 \langle \Delta E \rangle_d^{\text{SL}}$.

NTIS CRA&I		<input checked="" type="checkbox"/>
DHS TAB		<input type="checkbox"/>
Unannounced		<input type="checkbox"/>
Justification		
By		
Distribution/		
Availability Codes		
Dist	Avail and/or Special	
A-1		



i

Introduction

In a recent paper¹ (I), we discussed the parameterization of unimolecular reaction rates involving weak collisions of reactant molecules with a bath species. The collisional vibrational energy transfer efficiency β_c can be related to either of two average energy quantities conventionally used, namely, $\langle\Delta E\rangle_d$ and $\langle\Delta E\rangle_{all}$. The former is the collisional internal energy change averaged over the down transitions, while the latter is the step size averaged over both down and up transitions. Both quantities have been widely used in the literature, most recently by Barker and Golden² (BG). Oref³ has treated these quantities for the case, especially, of the Boltzmann model of collisional transition probabilities.

Gilbert⁴ has recently pointed out that $\langle\Delta E\rangle_d$ is the more appropriate quantity to use in parameterizing β_c ; indeed, this is the quantity which is implicit in the original Lindemann-Hinshelwood condition on collisional efficiency in their formulation of unimolecular reactions. Although the $\langle\Delta E\rangle_{all}$ quantity is directly accessible from even limited experiment, it has limited physical content. For good, comprehensive data,⁵ however, one can also extract $\langle\Delta E\rangle_d$ which is required for the specification of the correct form of the collisional transition probability function. Theoretical progress,⁶ in effect, is closely coupled to the further elucidation of this form.

It may be pointed out that the subject of weak gas collisions and their role in unimolecular reactions is not of relatively recent origin as is sometime supposed. These questions were entertained first in the late twenties, while in the thirties O.K. Rice and D.V. Sickman made quantitative weak collider calculations. In the early fifties, following the hiatus of World War II, H.S. Johnston and coworkers reinvigorated the whole question of the pressure, energy, and species dependence of the strength of collisions. A detailed review may be found in ref 5.

In I, we defined the quantity γ as the ratio $\langle \Delta E \rangle_{\text{all}} / \langle \Delta E \rangle_{\text{d}}$. The magnitude of γ depends strongly on the form of the collisional transition probability matrix \underline{P} that is appropriate (or selected). We may remind the reader that the stepladder (SL) and the exponential (EXP) models for the transition probabilities are the two types of models which have been used most prominently; the SL model may be considered as an approximation for the more physically apt gaussian (G) distribution. [More recently, a reverse exponential model has also been used^{2,4} and has properties similar to that of the SL and G models, although any deeper physical connotation of this form seems more obscure.] The SL and G models correspond to the physical case where large downjump transitions from the initial energy level are more probable than are very small transitions. While the EXP model corresponds to the reverse situation, where very small transitions have higher probability than larger transitions. It has been shown^{5,7} that the former model applies to cases where the behavior corresponds to stronger, more efficient collisions, and that the EXP model is more correct for very weak, inefficient collisions. As a rough rule of thumb, the dividing line between the two models of behavior corresponds to $\beta_c \approx 0.25$.

The magnitudes of $\langle \Delta E \rangle_{\text{d}}$ and $\langle \Delta E \rangle_{\text{all}}$ may be similar or quite disparate, depending upon the nature and conditions of a particular system, so that a relationship between the two is also desirable and necessary for the interpretation of literature results which may be cast in either form. The general and correct interconversion between these quantities is not facile. A relation was given by Troé^{8,9} for the EXP model as,

$$\langle \Delta E \rangle_{\text{all}} = \langle \Delta E \rangle_{\text{d}}^2 / (\langle \Delta E \rangle_{\text{d}} + F_E RT) \quad , \text{ where the density ratio } F_E \text{ is}$$

$$F_E = \left[\exp(E_0/RT) / RT \rho(E_0) \right] \int_{E_0}^{\infty} \rho(E) \exp(-E/RT) dE$$

F_E was emphasized to be near unity⁸, usually, although its deviation from unity was also shown.⁹ In fact, departure from unity is important under many experimental conditions.

BG have recently given a critique of Troe's earlier treatment^{8,9} for the EXP model and offered an improved correlation expression between the two energy parameters for both the EXP and SL cases. They used the Whitten-Rabinovitch (WR) approximation to give an expression for a desired vibrational eigenstate density ratio. Notwithstanding the obvious merit of the BG equations, it is very desirable to test other approximations that interrelate and rationalize these quantities. An iterative analytical procedure was developed in I for interrelating the two quantities for the case of the SL model. In this treatment, a classical expression for the density of vibrational states was employed in which the effective number of vibration modes $s'(E)$ was evaluated from the correct quantum statistical expression. Two useful temperature parameters, T_I the inversion temperature, and T_e the effective temperature were also introduced.

In the work described below, we have extended the comparison given in I between $\langle \Delta E \rangle_{all}$ and $\langle \Delta E \rangle_d$ to the EXP model case. Comparison of both models is also made with earlier literature expressions.

[We note, in response to a referee, that although the discussion here is couched in terms of reactive systems and illustrated below for systems at the level of the critical threshold energies, the conclusions derived are actually more general, of course, and apply to non-reactive systems, as well, and to any chosen energy level (such that the approximation conditions incorporated in our calculations are not violated).]

Calculational

Vibrational densities. Most of the calculations were made for the same prototype reactions as in I: the decomposition of nitryl chloride, and the isomerizations of methyl isocyanide, cyclopropane and cycloheptatriene (CHT). These reactants reflect differences in vibrational frequency patterns and molecular complexity, excitation levels and reaction temperatures (Table I).

The energy dependence of the density of vibrational states (E^{s-1} in the classical limit) can be parameterized either by adding the WR energy dependent correction term involving the zero point energy, i.e. $[E + a(E) E_2]^{s-1}$, or by taking s to be energy dependent, $s'(E)$; in the latter case, $s'(E)$ monotonically increases with energy to the maximum number of oscillators, s (note that internal rotations may be easily incorporated).

Exact calculations of reference densities as bench marks for all of the approximations examined here were made using densities based (arbitrarily) on the Haarhoff algorithm. No differences of any consequence arise in any of the calculations, figures, tables or conclusions presented below if, instead, WR densities are employed as reference values.

Collisional transition probabilities. The equations representing the down probabilities for the SL and EXP models are, respectively,

$$p_d^{SL} = p(E_i, E_j) = \text{const.}, \quad \text{for } E_j - E_i = \Delta E$$

$$= 0, \quad \text{for } E_j - E_i \neq \Delta E$$

and

$$p_d^{\text{EXP}} = p(E_i, E_j) = \text{const.} \exp \left[- (E_j - E_i) / \langle \Delta E \rangle_d \right], \quad \text{for } E_i \leq E_j$$

Up transition probabilities p_u are related to the down probabilities p_d by detailed balance and completeness:

$$\begin{aligned}
p_u(\Delta E)/p_d(\Delta E) &= p(E_i, E_j)/p(E_j, E_i) \\
&= \rho(E_i)/\rho(E_j) \exp[-\Delta E/RT] \quad , \Delta E = |E_i - E_j| ; \quad (1)
\end{aligned}$$

$$\sum_{\text{all } E_i} p(E_i, E_j) = 1$$

It is convenient to render eq. (1) into the form,

$$p_u(\Delta E)/p_d(\Delta E) = \exp(-\Delta E/RT_e) ;$$

which requires that the density ratio take the form , $\rho(E_i)/\rho(E_j) = \exp(c\Delta E)$; where T_e is an effective temperature given by

$$T_e = T/(1 - cRT) \quad (2)$$

Table 1 illustrates the density ratio as a function of ΔE for various reactants, at $E_i = E_0$. Of prime importance is the near-linearity of the log of the density ratio with increase of ΔE . By parameterizing $\rho(E)$ as $E^{s'(E)-1}$ in I, the relation $\ln(\rho(E+\Delta E)/\rho(E)) = (s'(E)-1)\ln(1+\Delta E/E)$ was used. In this paper, we will call the fitted classical approximation, designated as TR, as the $s'(E)$ value which makes

$$\ln(\rho(E + \langle \Delta E \rangle_d)/\rho(E)) = (s'(E) - 1) \langle \Delta E \rangle_d / E \quad (3)$$

$$= c_{TR} \Delta E \quad \text{for } SL$$

$$= c_{TR} \langle \Delta E \rangle_d \quad \text{for } EXP, \quad \text{with } \langle \Delta E \rangle_d / E \ll 1.$$

Alternatively, BG have used other parameterization, namely, the WR expression whereby

$$\begin{aligned}
\ln \frac{\rho(E+\Delta E)}{\rho(E)} &= (s-1) \ln \left[\frac{E + a(E+\Delta E)E_z}{E + a(E)E_z} + \frac{\Delta E}{E + a(E)E_z} \right] \\
&\approx (s-1) \ln \left(1 + \frac{\Delta E}{E + a(E)E_z} \right) \approx \frac{(s-1)\Delta E}{E + a(E)E_z} = c_{WR} \Delta E
\end{aligned} \quad (4)$$

This compact formulation has been made to depend on only a single correction constant, $a(E)$.

Average energy quantities. The average energy quantities may be expressed in terms of the transition probabilities

$$\langle \Delta E \rangle_u = \sum_{E_j > E_i} (E_j - E_i) p(E_j, E_i) / \sum_{E_j > E_i} p(E_j, E_i)$$

$$\langle \Delta E \rangle_d = - \sum_{E_j \leq E_i} (E_j - E_i) p(E_j, E_i) / \sum_{E_j \leq E_i} p(E_j, E_i)$$

$$\langle \Delta E \rangle_{all} = \bar{p}_u \langle \Delta E \rangle_u - \bar{p}_d \langle \Delta E \rangle_d$$

where,

$$\bar{p}_u = \sum_{E_j > E_i} p(E_j, E_i) \quad \text{and} \quad \bar{p}_d = \sum_{E_j \leq E_i} p(E_j, E_i)$$

These expressions take an obvious simplified form for the SL model.

The sign convention makes $\langle \Delta E \rangle_{all} = -\langle \Delta E \rangle_d$ when $p_d \rightarrow 1$, and $\langle \Delta E \rangle_{all} = \langle \Delta E \rangle_u$ when $p_d \rightarrow 0$. Both $\langle \Delta E \rangle_u$ and $\langle \Delta E \rangle_{all}$ are strongly dependent on molecular complexity and temperature for a given $\langle \Delta E \rangle_d$.

The temperature quantities, T_e and T_I . The ratio p_u/p_d is related to ΔE through T_e which is independent of ΔE for c constant. The condition in eq. (3) is that $\langle \Delta E \rangle_d \ll E$; in eq. 4, the condition is $\langle \Delta E \rangle_d \ll (E + a(E)E_2)$.

For molecules of given energy, e.g. E_o , an inversion temperature T_I was defined in I as the temperature at which $\langle \Delta E \rangle_{all} = 0$ i.e. $\langle \Delta E \rangle_d = \langle \Delta E \rangle_u$, or,

$$- \sum_{E_j < E_i} (E_j - E_i) p(E_j, E_i) = \sum_{E_j > E_i} (E_j - E_i) p(E_j, E_i) \quad (5a)$$

For this constraint, the Boltzmann factors are offset by the density ratios. With a stepladder probability model at energy E_o , this constraint was satisfied (cf. I) when, from eq. 3,

$$T_I = \Delta E / \ln(\rho(E_o + \Delta E) / \rho(E_o)) R = E_o / (s'(E) - 1) R.$$

Consider the general limiting cases for T_e (eq. 2):

$$cRT \gg 1, \quad T_e = -1/cR$$

$$cRT \ll 1, \quad T_e = T$$

For the fitted classical approximation,

$$\text{when } c_{TR}RT = 1, \quad T_e^{TR} = \infty; \quad \text{so } T = T_I^{TR} = E_o / (s'(E) - 1)R \quad (5b)$$

In the limit, $T \ll T_I^{TR}$ (i.e. $c_{TR}RT \ll 1$), i.e. at low temperatures and/or high E_o , $T = T_e^{TR}$; in this limit, $p_u < p_d$, the maximum in the Boltzmann distribution is below E_o and down transitions dominate. For the case, $T \gg T_I^{TR}$ ($c_{TR}RT \gg 1$), i.e. at very high temperatures, the maximum in the Boltzmann distribution is above E_o and up transitions dominate.

We may now derive specific expressions from these general results for the EXP model and recall expressions from I for the SL case. The expressions are for the energy origin $E_i = E_o$, but are valid for any E so long as $\langle \Delta E \rangle_d \ll E$ for the EXP model.

Stepladder model. For the SL model, we showed in I that

$$\begin{aligned} p_u/p_d &= \exp(-\Delta E/RT_e) \\ \gamma^{SL} &= - (1 - \exp[-\Delta E/RT_e]) / [1 + \exp(-\Delta E/RT_e)] \\ &= -\tanh(\Delta E/2RT_e) \end{aligned} \quad (6)$$

Thus $\langle \Delta E \rangle_d$ and $\langle \Delta E \rangle_{all}$ are universally related via T_e . The validity of the approximations in using T_e , i.e. in using a constant T_I , is illustrated in Table 2 where values of T_I are presented; T_I is nearly independent of step size: there is a slight increase in T_I with an increase in step size since the increase in density ratio with energy does not completely compensate for the decrease in the Boltzmann factor. It is evident that a complex molecule (large s) with a large E_o will have a comparable T_I to a smaller molecule with a small E_o , i.e. $(s-1)/E_o$ constant; e.g. C_3H_6 and CH_3NC (Table 2).

Exponential model. For the EXP model

$$\begin{aligned}
 \langle \Delta E \rangle_{\text{all}} &= \sum_{E_j} (E_j - E_i) p(E_j, E_i) \\
 &= \frac{\sum_{E_j \leq E_i} (E_j - E_i) \exp[-(E_i - E_j)/\langle \Delta E \rangle_d] + \sum_{E_j > E_i} (E_j - E_i) \exp[-(E_j - E_i)/\langle \Delta E \rangle_d] \cdot \rho(E_j) \exp[-(E_j - E_i)/RT] / \rho(E_i)}{\sum_{E_j \leq E_i} \exp[-(E_i - E_j)/\langle \Delta E \rangle_d] + \sum_{E_j > E_i} \exp[-(E_j - E_i)/\langle \Delta E \rangle_d] \cdot \rho(E_j) \exp[-(E_j - E_i)/RT] / \rho(E_i)} \\
 &= \frac{\sum_{\Delta E > 0} \Delta E [-1 + \exp(-\Delta E/RT_e)] \exp(-\Delta E/\langle \Delta E \rangle_d)}{1 + \sum_{\Delta E > 0} [1 + \exp(-\Delta E/RT_e)] \exp(-\Delta E/\langle \Delta E \rangle_d)} \quad (7)
 \end{aligned}$$

In the evaluation of eq. 7, the grain size G (which corresponds to the minimum step size) was taken sufficiently small, and the number of steps included in the EXP model sufficiently large so that convergence was obtained. In these calculations, for the grain size, $G = \langle \Delta E \rangle_d / 256$, and an energy limit of $16 \langle \Delta E \rangle_d$ (i.e. 4096 steps), absolute convergence was found to within 0.2% in the worst case and was $< 0.1\%$ in most cases; the error for the ratios of sums is even less. In the limit, $\Delta E \rightarrow 0$, the sums in eq. 7 can be replaced with an integral as done by Troe and by BG. Integration gives

$$\langle \Delta E \rangle_{\text{all}} = - \langle \Delta E \rangle_d^2 / (\langle \Delta E \rangle_d + RT_e)$$

and

$$\gamma_{\text{TR}}^{\text{EXP}} = - \langle \Delta E \rangle_d / (\langle \Delta E \rangle_d + RT_e^{\text{TR}}) \quad (8a)$$

where $T_e^{\text{TR}} = T / (1 - (s'(E) - 1)RT/E_0)$, since $T_e^{\text{TR}} = T / (1 - T/T_I^{\text{TR}})$. (8b)

Earlier, Troe^{8,9} has used,

$$\langle \Delta E \rangle_{\text{all}} = - \langle \Delta E \rangle_d^2 / (\langle \Delta E \rangle_d + F_E RT)$$

so,

$$\gamma_T^{\text{EXP}} = - \langle \Delta E \rangle_d / (\langle \Delta E \rangle_d + F_E RT) \quad (9)$$

where F_E was given as positive and was evaluated with use of the WR approximation.

BG gave the relation,

$$\langle \Delta E \rangle_{\text{all}} = \left[\frac{1}{\langle \Delta E \rangle_d} + \frac{1}{RT} - \frac{(s-1)}{E + a(E)E_z} \right]^{-1} - \langle \Delta E \rangle_d$$

We may simplify this equation by writing

$$\gamma_{BG}^{\text{EXP}} = -\langle \Delta E \rangle_d / (\langle \Delta E \rangle_d + RT_e^{\text{BG}}) \quad (10)$$

where,

$$T_e^{\text{BG}} = T / \left(1 - (s-1)RT / (E + a(E)E_z) \right) = T / (1 - T/T_I^{\text{BG}})$$

These γ^{EXP} expressions (eqs. 8a, 9 and 10) are equivalent when $F_E^T = T_e^T = T_e^{\text{TR}} = T_e^{\text{BG}}$; this condition is realized for small molecules at low temperatures. The general behavior is illustrated in Table 3. For a large molecule and higher temperatures, the aberration of $F_E = T_e^T/T$ from $T_e(\text{exact})/T$ is striking.

For an EXP model, eq. 5a takes the form

$$\sum_{\Delta E > 0} \Delta E \exp(-\Delta E / \langle \Delta E \rangle_d) = \left[\sum_{\Delta E > 0} \Delta E \exp(-\Delta E / \langle \Delta E \rangle_d) \cdot (\rho(\varepsilon + \Delta E) / \rho(\varepsilon)) \exp(-\Delta E / RT) \right]$$

under the condition, $T \equiv T_I^{\text{EXP}}$. This equation may be solved iteratively for T_I^{EXP} . A listing of values is given in Table 2. It is noted that T_I^{EXP} are somewhat larger than those calculated for the SL model and increase somewhat faster with $\langle \Delta E \rangle_d$ than for the SL model. In effect a higher temperature is required to offset the decrease in p_u due to the higher weighting of the small step sizes (head of the distribution) characteristic of the EXP model.

Results and Discussion

SL and EXP model calculations were performed for the four reactions over the temperature range 250 K to 4000 K with average step sizes ranging from 100 to 1600 cm^{-1} . For comparative purposes, ethyl bromide and methyl cycloheptatriene calculations were also performed for two temperatures and two step sizes each. Results for these compounds are in good agreement with those published by Gilbert⁴. Our ethyl bromide results at 1000 K are in agreement with the corrected values of Gilbert (private communication).

Step ladder model. Results are summarized in Fig 1 where γ^{SL} is plotted as a function of the reduced parameter, E'_e , defined as $\langle \Delta E \rangle_d / RT_e^{TR}$. By calibration of $s'(E_0 + \Delta E)$ for every ΔE , the slight scatter shown in Fig 2 of I has been removed; the calculations follow eq. 6. As expected, γ^{SL} increases from -1, for large $\langle \Delta E \rangle_d$ and/or low temperature, to 0, for small $\langle \Delta E \rangle_d$ and/or high temperature, and continues to increase for temperatures greater than T_I as $\langle \Delta E \rangle_d$ increases. At temperatures greater than T_I , up transitions dominate and $\langle \Delta E \rangle_{all}$ approaches $\langle \Delta E \rangle_u$ in magnitude, i.e. $\gamma^{SL} = 1$. For most small reactants, the region where $\gamma^{SL} > 0$ is not experimentally accessible. For CHT, T_I was realized experimentally by Troe, et. al.¹⁰

When $E'_e < 0.2$, γ^{SL} is linear with E'_e ; the slope is -0.5. This observation is verified by expanding eq. (6) which gives,

$$\gamma^{SL} = -\Delta E / 2RT_e = -E'_e / 2$$

Comparison of this expression with the limiting form of eq. 8a, gives the relation $\langle \Delta E \rangle_d^{EXP} = \Delta E_d^{SL} / \sqrt{2}$, for a given (experimental) determination of $\langle \Delta E \rangle_{all}$.

Exponential Model. The results for the EXP model are illustrated in Fig 1. The scatter is greater than for the SL model, but the fit is remarkably good. The deviations are due to the large energy range that is spanned by the energy transitions. The behavior for $\gamma^{EXP} < 0$ is qualitatively similar to the SL model; major differences occur at low E'_e ; γ^{EXP} is linear with E'_e with a slope of -1 and not -0.5, as for SL. For larger E'_e , γ^{EXP} approaches -1 more slowly than does γ^{SL} . For $E'_e < 0$, γ^{EXP} exceeds unity. This results from the fact that the Boltzmann temperature factor is less important than the density ratio increase; larger steps are enhanced.

A comparison of γ^{SL} and γ^{EXP} is illustrated in Fig 2. For sufficiently large E'_e , $\langle \Delta E \rangle_{all}^{SL} = \langle \Delta E \rangle_{all}^{EXP} = -\langle \Delta E \rangle_d$. As E'_e decreases, $\langle \Delta E \rangle_{all}$ for the EXP

model does not increase as fast as the SL model; as $E'_e \rightarrow 0$, the reverse becomes true, hence the minimum in Fig 2. This behavior can be understood by looking at the limiting forms of eq. 7 incorporated in γ^{EXP} .

For small E'_e , the quantity $\exp(-\Delta E/RT_e)$ may be expanded in linear form and the summation is over a distribution which depends on the second moment of ΔE , i.e. favors the tail of the energy step distribution corresponding to larger steps. When this sum is compared to a SL model a factor of 2 results (the limit of eq. 6).

For large E'_e , $\exp(-\Delta E/RT_e)$ is close to 0, and the resulting sum in eq. 7 has only a linear term in ΔE , so that the head of the energy step distribution dominates; a smaller average step size results. For $E'_e > 3$, γ^{EXP} approaches -1 more slowly than does γ^{SL} , with increasing E'_e .

We note that the behavior in Fig 2 is reminiscent of the variation of the relative magnitudes of β_c^{EXP} and β_c^{SL} taken as a function of $E' (= \langle \Delta E \rangle_d / \langle E^* \rangle)$ (a parameter similar in nature to E'_e) which was described by us some time ago.¹¹ Plots of β_c vs E' given there for both models do not coincide at low values of E' but cross and converge as E' increases. This behavior can and has been used⁵ to differentiate transition probability models and their domain of relevance. In ref 11, the plots of β_c vs E' separate by a factor of $\sim \sqrt{2}$ at small values of E' . This is a positive feature that assists in the experimental determination of the correct form of β_c , and is not a shortcoming as misstated by Troe.⁹

Comparison with previous work. The present results may be compared to the γ functions presented by Troe⁹ and BG. As pointed out by BG, Troe's function (eq. 9) suffers from the qualitative defect that it cannot provide $\gamma^{\text{EXP}} > 0$. Both $\gamma_{\text{TR}}^{\text{EXP}}$ (eq. 8a) and $\gamma_{\text{BG}}^{\text{EXP}}$ (eq. 10) allow for $\gamma^{\text{EXP}} > 0$, since T_e

can be less than zero. This behavior may be analyzed in more detail as follows. Equations 8a, 9 and 10 can be recast into the form

$$\gamma^{\text{EXP}}(E'_e) = -E'_e / (1 + E'_e) \quad (11a)$$

For eq. 8a, $E'_e = \langle \Delta E \rangle_d / RT_e^{\text{TR}}$, and $T_e^{\text{TR}}/T = 1/(1 - T/T_I^{\text{TR}})$; (11b)

for eq. 10, $E'_e = \langle \Delta E \rangle_d / RT_e^{\text{BG}}$, and $T_e^{\text{BG}}/T = 1/(1 - T/T_I^{\text{BG}})$; (11c)

and, for eq. 9, $E'_e = \langle \Delta E \rangle_d / RT_e^{\text{T}}$, and $T_e^{\text{T}}/T = F_E$

For sufficiently low temperature, the quantities T_e^{TR}/T , T_e^{BG}/T and F_E are all nearly linear with temperature. At higher temperatures, only T_e^{TR}/T and T_e^{BG}/T display similar coefficients of higher powers of T . Also, when $T > T_I$, T_e^{T}/T remains positive while T_e^{TR}/T and T_e^{BG}/T become negative as required physically. A tabulation of the T_e/T quantities is given in Table 3 for the conditions of the present calculations.

The relative merits of the various T_e/T quantities for parameterizing γ^{EXP} can be found by defining

$$R_\gamma = \left| \frac{\Delta \gamma^{\text{EXP}}}{\gamma^{\text{EXP}}} \right| = \left| \frac{\gamma^{\text{EXP}}(E'_e) - \gamma^{\text{EXP}}(\text{exact})}{\gamma^{\text{EXP}}(\text{exact})} \right|$$

The resulting values of R_γ for the various approximations are displayed in Fig. 3 for two systems (CH_3NC and CHT) over a range of temperature and step sizes, although calculations were made for all four molecules. To avoid display of three scales for the abscissa, the comparison of the approximations is shown for the same values of $E'_e(\text{TR})$, although the appropriate value of $E'_e(\text{BG})$ and $E'_e(\text{T})$ were used in calculating $\gamma_{\text{BG}}^{\text{EXP}}$ and $\gamma_{\text{T}}^{\text{EXP}}$ from eq. 11a. The comparison is correct since points related vertically in the figure do correspond to the same values of T , $\langle \Delta E \rangle$ and given molecule. To be noted is

the increasing deviation of R_γ for all three approximations as E_e' decreases; this occurs for either a decrease in step size and/or an increase in temperature. For a given E_e' , R_γ increases with molecular complexity ($\text{CHT} > \text{CH}_3\text{NC}$). For all calculations, the R_γ deviations are largest for Troe's approximation; hence eq. 9 with F_E is not recommended. TR values are better than are BG, and this improvement is only slightly reduced if $s'(E)$ were to be used as a constant average value independent of $\langle \Delta E \rangle$.

For the case of the EXP model, the BG calculations require the fewest number of function evaluations. Because of the large experimental error in measured quantities, $\langle \Delta E \rangle_d$ or $\langle \Delta E \rangle_{all}$, we advocate that the BG approximation be used unless greater calculational precision is desired, in which case γ^{EXP} (exact) may be computed readily (indeed, all the calculations for this paper were performed on an IBM-PC)

An interesting comparison may be added. Both Troe and BG derived eqs. 9 and 10 by assuming $a(E) = a(E_0)$; this approximation, although not generally justified, is appropriate for small molecules with $E \approx E_0$. Troe then performed an analytical integration to determine $F_e (= T_e^T/T)$; BG, on the other hand, before integration introduced a fortunate second approximation $\ln(1 + \Delta E / (E_0 + a(E_0)E)) \approx \Delta E / (E_0 + a(E_0)E_2)$ with result:

$$\ln\left(\frac{E_0 + a(E)E_2}{E_0 + a(E_0)E_2} + \frac{\Delta E}{E_0 + a(E_0)E_2}\right) \approx \ln\left(1 + \frac{\Delta E}{E_0 + a(E_0)E_2}\right) \approx \frac{\Delta E}{E_0 + a(E_0)E_2},$$

and with near-compensation of errors introduced by the first approximation. (See Appendix).

A comparison of γ^{SL} calculations analogous to the above between TR and BG is superfluous for δ -function transitions. In effect, our fitted classical approximation was made exact for any initial energy E_i .

Interrelation of $\langle \Delta E \rangle_d$ and $\langle \Delta E \rangle_{all}$. The transformation from $\langle \Delta E \rangle_d$ to $\langle \Delta E \rangle_{all}$ is straight forward: i) T_I is first computed by eq. 5b; ii) T_e is evaluated for the specific temperature (eq. 11b); iii) E_e' is calculated from

$\langle \Delta E \rangle_d / RT_e$ and used in eq. 6 or eq. 11a to solve for γ^{SL} or γ^{EXP} . Finally, $\langle \Delta E \rangle_{all} = \gamma \cdot \langle \Delta E \rangle_d$ for either case.

The reverse process, to derive $\langle \Delta E \rangle_d$ from $\langle \Delta E \rangle_{all}$ for the EXP case, utilizes the expression (from eq. 11a)

$$\langle \Delta E \rangle_d = \frac{-\langle \Delta E \rangle_{all}}{2} \left[1 + \sqrt{1 - 4RT_e / \langle \Delta E \rangle_{all}} \right]$$

for the EXP case. As described in I, an iteration technique is used to determine $\langle \Delta E \rangle_d$ for the SL model.

At the request of a referee we are including Figure 4 where $\gamma^{EXP}(\text{exact})$ is plotted as a function of temperature for the methyl isocyanide and cycloheptatriene systems. Step sizes of 100 and 1600 cm^{-1} are illustrated. Values of $\gamma^{EXP}(\text{exact})$ for intermediate step sizes and/or other reactants can be found by interpolation. These family of curves illustrate the advantage of incorporating molecular complexity, step size and temperature in the reduced parameter E'_e so that a quasi-universal curve results.

Conclusion

A critique has been given of the various parameters that enter into the formulation of collisional efficiency for transfer of vibrational energy. The ratio $\gamma = \langle \Delta E \rangle_{all} / \langle \Delta E \rangle_d$ has been evaluated. A reduced energy transfer quantity, $E'_e = \langle \Delta E \rangle_d / RT_e$, was introduced so that γ^{SL} and γ^{EXP} can be calculated from universal functions for E'_e . These functions exhibit different limiting forms for the EXP and SL models.

Comparison with exact calculations has been made for the present use of a fitted classical approximation and for two earlier treatments in the literature that employed the WR approximation. Although the present approximation is relatively more accurate, in general, the treatment of Barker and Golden is very adequate for many systems and conditions and is simpler to use. Actually, exact calculations are not arduous and are also advocated.

Acknowledgment

We thank the Office of Naval Research and the National Science Foundation for their support.

References

1. D.C. Tardy, B.S. Rabinovitch, J. Phys. Chem. 1985, 89,
2. J. R. Barker, R.E. Golden, J. Phys. Chem. 1984, 88, 1012.
3. I. Oref, J. Chem. Phys. 1982, 77, 5146 and later papers.
4. R. G. Gilbert, Chem. Phys. Lett. 1983, 96, 259.
5. D.C. Tardy, B.S. Rabinovitch, Chem. Rev. 1977, 77, 369.
6. R.G. Gilbert, J. Chem. Phys. 1984, 80, 5501.
7. G. H. Kohlmaier, B.S. Rabinovitch, J. Chem. Phys. 1963, 38, 1692, 1709.
8. J. Troe, Ber. Bunsenges, Phys. Chem. 1973, 77, 665.
9. J. Troe, J. Chem. Phys. 1977, 66, 4745, 4758.
10. D.C. Astholz, J. Troe and W. Wieters, Proc. 12th Internat. Sympos. Shock Tubes, Jerusalem, 1979, p. 607 and J. Chem. Phys. 1979, 70, 5107.
11. D.C. Tardy, B.S. Rabinovitch, J. Chem. Phys. 1966, 45, 3720; 1968, 48, 1282.

Table 1: Reactant Parameters and Calculated Quantities

Reactant	E_0 (cm^{-1})	T(K) ^a	μ	$s'(E_0)$	$a(E_0)$	E_z (cm^{-1})	$\rho E_0 + \Delta E / \rho E_0$				
							$\Delta E'$ (cm^{-1})	100	200	400	800
NU_2Cl^b	10325	450-525 ^d	6	5.1	0.910	2600	1.040	1.081	1.167	1.355	1.803
CH_3NC^b	13300	550-825 ^e	12	7.9	0.964	9626	1.053	1.118	1.226	1.498	2.210
$c\text{-C}_3\text{H}_6^b$	21875	700-1800 ^f	21	13.2	0.904	17165	1.057	1.118	1.248	1.554	2.389
$c\text{-C}_7\text{H}_8^c$	18000	650-1400 ^g	39	20.0	0.845	26105	1.111	1.233	1.518	2.292	5.420

a) Experimental thermal reaction temperatures

b) Vibrational frequencies from ref 11

c) Vibrational frequencies as reported by M.V. Evans and R.C. Lord, J. Amer. Chem. Soc. 1960, 82, 1876.

d) K.A. Holbrook, Royal Chem. Soc. (London) Annual Revs. 1984, 163.

e) A. Lifshitz, H.F. Carroll and S.H. Bauer, J. Amer. Chem. Soc. 1964, 86, 1488.

f) J.N. Bradley and M.A. Friend, Trans. Far. Soc. 1971, 67, 72

g) from ref. 10

Table 2 Inversion Temperatures T_I (exact)

Reactant	$\langle \Delta E \rangle_d$ (cm^{-1})											
	100		200		400		800		1600			
	SL	EXP	SL	EXP	SL	EXP	SL	EXP	SL	EXP	SL	EXP
NO_2Cl	3690	3719	3705	3761	3734	3844	3791	3998	3904	4274		
CH_3NC	2799	2813	2806	2833	2820	2874	2848	2950	2903	3088		
$c\text{-C}_3\text{H}_6$	2585	2593	2589	2605	2597	2628	2613	2672	2644	2753		
$c\text{-C}_3\text{H}_8$	1372	1376	1374	1383	1379	1396	1388	1422	1406	1467		

Table 3 Reduced Temperature (T_e/T) for EXP model

Reactant $\langle \Delta E \rangle_d$ (cm^{-1})	T(K)											
	250				500				1000			
	$\frac{T_e^{TR}}{T}$	$\frac{T_e^{BG}}{T}$	$\frac{T_e^T}{T}$	$\frac{T_e^{a(\text{exact})}}{T}$	$\frac{T_e^{TR}}{T}$	$\frac{T_e^{BG}}{T}$	$\frac{T_e^T}{T}$	$\frac{T_e^{(\text{exact})}}{T}$	$\frac{T_e^{TR}}{T}$	$\frac{T_e^{BG}}{T}$	$\frac{T_e^T}{T}$	$\frac{T_e^{(\text{exact})}}{T}$
CH ₃ NC	1 099	1 095	1 094	1 097	1 220	1 210	1 205	1 219	1 563	1 530	1 497	1 569
	1 095	1 095	1 094	1 103	1 218	1 210	1 205	1 217	1 532	1 530	1 497	1 535
CHI	1 224	1 197	1 196	1 223	1 577	1 492	1 483	1 569	3 725	2 935	2 719	3 745
	1 217	1 197	1 196	1 220	1 552	1 492	1 483	1 568	3 493	2 935	2 719	3 382
CH ₃ NC	2 176	2 082	1 927	2 188	1500				$\frac{T_e^{TR}}{T}$	$\frac{T_e^{BG}}{T}$	$\frac{T_e^T}{T}$	$\frac{T_e^{(\text{exact})}}{T}$
	2 087	2 082	1 927	2 043					3 580	3 258	2 586	3 525
CHI	-10 273	89 997 ^b	8 001	-10 683	2000				$\frac{T_e^{TR}}{T}$	$\frac{T_e^{BG}}{T}$	$\frac{T_e^T}{T}$	$\frac{T_e^{(\text{exact})}}{T}$
	-14 179 ^b	89 997 ^b	8 001	-42 504					-2 159	-3 140	56 04	-2 184

a) $T_e(\text{exact})$ obtained by using $\gamma^{\text{EXP}}(\text{exact})$ in eq. 11a and $T_e(\text{exact}) = \langle \Delta E \rangle_d / (RE'_e)$.

b) Peculiar accidental values that arise from eqs. 11b and 11c as $1 - T/T_I \rightarrow 0$; the transition of T_e/T goes to negative values through infinity and all these values of T_e^{TR}/T or T_e^{BG}/T are closer to $T_e(\text{exact})/T$ than are T_e^T/T .

Appendix

It seems useful to summarize the nature of the approximations involved in the T and BG formulations. Equation 7 with $E=E_0$ can be written as

$$\langle \Delta E \rangle_{all} = \frac{c1 \langle \Delta E \rangle_{up} + c2 \langle \Delta E \rangle_{down}}{c1 + c2} \quad (A1)$$

where

$$c1 = - \sum_{\Delta E > 0} \Delta E \exp(-\Delta E / \langle \Delta E \rangle_{up})$$

$$c2 = \sum_{\Delta E > 0} \Delta E \exp(-\Delta E / \langle \Delta E \rangle_{down}) D(\Delta E) \exp(-\Delta E / \langle \Delta E \rangle_{down})$$

$$c3 = \sum_{\Delta E > 0} \exp(-\Delta E / \langle \Delta E \rangle_{down})$$

$$c4 = \sum_{\Delta E > 0} \exp(-\Delta E / \langle \Delta E \rangle_{up}) D(\Delta E) \exp(-\Delta E / \langle \Delta E \rangle_{up})$$

where $D(\Delta E) = \rho(E_0 + \Delta E) / \rho(E_0)$

The sign change in $\langle \Delta E \rangle_{all}$ occurs when $c1=c2$, i.e. when $\langle \Delta E \rangle_{down} = \langle \Delta E \rangle_{up}$.

Troe's expression for F_E was developed to take into account the energy dependence of the density of states ratio in parameterizing thermal unimolecular rate constants in the second order region. As a result there is very little resemblance to the form given in equation (A1); the competition between "up" and "down" transitions and the details of the "down" probabilities are absent.

Using the Whitten-Rabinovitch approximation the density ratio, $D(\Delta E)$ can be simplified by assuming $a(E)$ is a constant independent of energy. With just this constancy assumption $D(\Delta E)$ is given by A2;

$$D_C(\Delta E) = \left(1 + \frac{\Delta E}{(E_0 + a(E_0)E_2)} \right)^{S-1} \quad (A2)$$

by further assuming that

$$\ln \left(1 + \frac{\Delta E}{(E_0 + a(E_0)E_2)} \right) = \frac{\Delta E}{E_0 - a(E_0)E_2}$$

as done by BG equation A3 results:

$$D_{BG}(\Delta E) = \exp \left(\frac{(-1)\Delta E}{(E_0 + a(E)E_2)} \right) \quad (A3)$$

Expression A2 produces $D_C(\Delta E) < D(\Delta E)$ for all ΔE ; the difference increases with increasing ΔE and/or molecular complexity. On the other hand when A3 is used $D_{BG}(\Delta E) < D(\Delta E)$ for small ΔE and for large ΔE $D_{BG} > D(\Delta E)$; the crossover point is $\Delta E \sim 1700 \text{ cm}^{-1}$ for methyl isocyanide and increases with molecular complexity.

Expression A3 is a better approximation to the true density ratio for all values of ΔE . Thus the approximation for the constancy of $a(E)$ which underestimates $D(\Delta E)$ is compensated by the over estimate in using only the linear term for the expansion of $\ln(1 + x)$.

The approximations used for $D(\Delta E)$ will determine the value of $\langle \Delta E \rangle_{all}$ (eq. A1) and γ^{EXP} ; Table A1 is a summary of calculational results for representative systems, step sizes and temperatures. As expected from the form of F_E , γ_T^{EXP} shows the largest deviation from $\gamma^{EXP}(\text{exact})$. The inadequacy of A2 for $D(\Delta E)$ is shown by comparing γ_{A2}^{EXP} and γ_{A3}^{EXP} ; for increasing step size and/or molecular complexity the difference between these quantities increases. The difference between the integral approximation by BG (γ_{BG}^{EXP}) and the summations used in equation A1 (γ_{A3}^{EXP}) is negligible and for practical purposes can be ignored. The goodness of the BG approximations as illustrated in Fig 3 depends on molecular complexity, step size and temperature in a complex manner; in general the BG approximation becomes inadequate for small values of E_0' . For a given E_0' the difference increases with molecular complexity.

Table A1: Calculated Values of γ^{EXP}

System	$\langle \Delta E \rangle$ (cm^{d-1})	T (K)	EXP ^a γ_{exact}	EXP ^b γ_T	EXP ^c γ_{BG}	EXP ^d γ_{A3}	EXP ^e γ_{A2}
CH ₃ NC	100	250	-0.343	-0.345	-0.345	-0.344	-0.344
		500	-0.191	-0.193	-0.192	-0.192	-0.192
		1000	-0.084	-0.088	-0.086	-0.086	-0.086
		1500	-0.042	-0.047	-0.044	-0.044	-0.044
		2000	-0.020	-0.027	-0.022	-0.022	-0.022
	1600	250	-0.883	-0.894	-0.894	-0.883	-0.883
		500	-0.786	-0.793	-0.792	-0.787	-0.783
		1000	-0.598	-0.606	-0.601	-0.599	-0.603
		1500	-0.428	-0.443	-0.424	-0.423	-0.436
		2000	-0.274	-0.308	-0.261	-0.261	-0.287
CHT	100	250	-0.319	-0.325	-0.325	-0.324	-0.324
		500	-0.154	-0.163	-0.162	-0.161	-0.162
		1000	-0.037	-0.050	-0.047	-0.047	-0.047
		1500	0.009	-0.012	-0.001	-0.001	-0.001
		2000	0.034	-0.001	0.023	0.023	0.023
	1600	250	-0.873	-0.885	-0.885	-0.875	-0.875
		500	-0.743	-0.756	-0.755	-0.751	-0.752
		1000	-0.405	-0.458	-0.440	-0.439	-0.451
		1500	0.037	-0.161	-0.017	-0.017	-0.082
		2000	0.578	-0.020	0.579	0.578	0.353

- a) Exact γ using $\langle \Delta E \rangle_{a11}$ calculated from equation (A1).
- b) γ calculated using equation 9.
- c) γ calculated using equation 10.
- d) γ calculated using equations (A1) and (A3) [constancy of $a(E)$ and linear expansion for $\ln(1+x)$].
- e) γ calculated using equations (A1) and (A2) [constancy of $a(E)$].

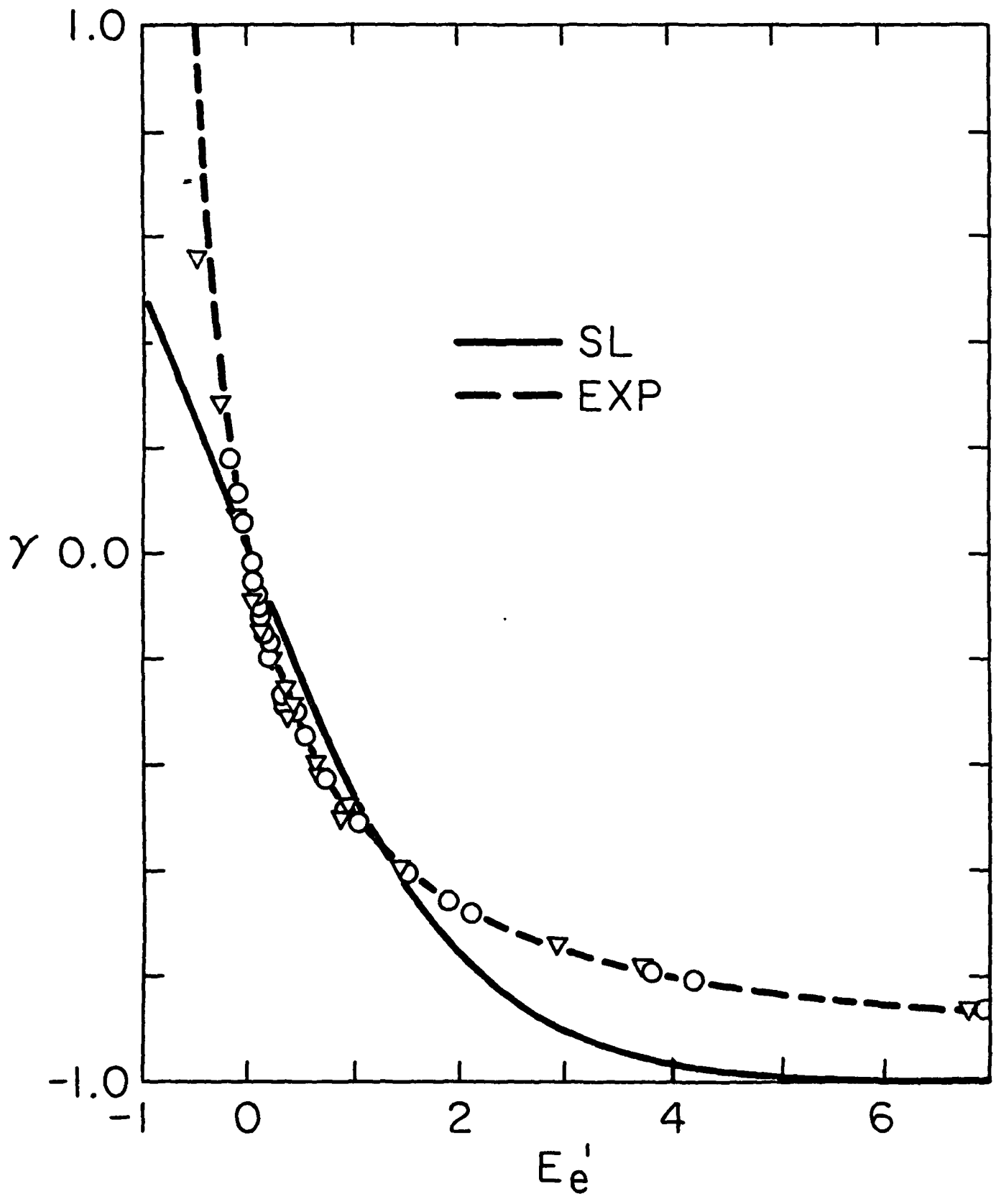
Figure Captions

Fig 1: Plots of $\gamma^{\text{SL}}(\text{exact})$ [solid line] and $\gamma_{\text{TR}}^{\text{EXP}}$ (eq. 8a [broken line]) vs E'_e ($=\langle\Delta E\rangle_d/RT^{\text{TR}}$) for nitryl chloride, methyl isocyanide, cyclopropane, and cycloheptatriene with step sizes of 100, 200, 400, 800 and 1600 cm^{-1} , each at 250 K, 500 K, 1000 K, 2000 K and 4000 K. Equation 11b in text was used to calculate T_e^{TR} . For clarity of viewing, only data points for CH_3NC (circles) and cycloheptatriene (triangles) are shown for $\gamma_{\text{TR}}^{\text{EXP}}$ (exact). All calculated points for $\gamma_{\text{TR}}^{\text{SL}}$ lie on the $\gamma^{\text{SL}}(\text{exact})$ curve.

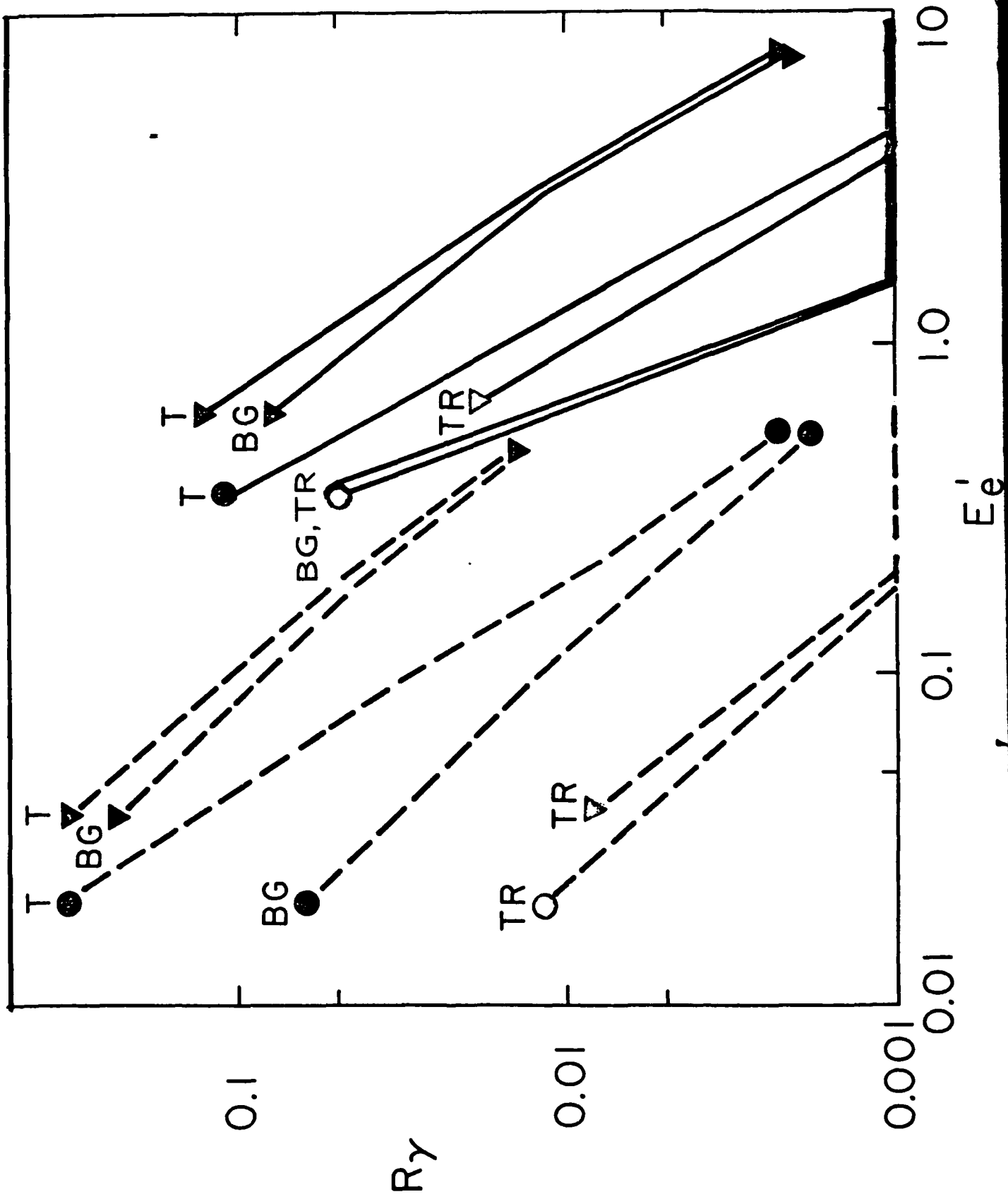
Fig 2: Plots of $\gamma_{\text{TR}}^{\text{EXP}} / \gamma_{\text{TR}}^{\text{SL}}$ [solid line] and data points for $\gamma^{\text{EXP}}(\text{exact}) / \gamma^{\text{SL}}(\text{exact})$ vs E'_e ($=\langle\Delta E\rangle_d/RT^{\text{TR}}$) for reactants and conditions specified for Fig. 1; where $\gamma_{\text{TR}}^{\text{EXP}} / \gamma_{\text{TR}}^{\text{SL}} = (E'_e / (1 + E'_e)) / ((1 - \exp(-E'_e)) / (1 + \exp(-E'_e)))$ as derived from eqs. 6 and 8a.

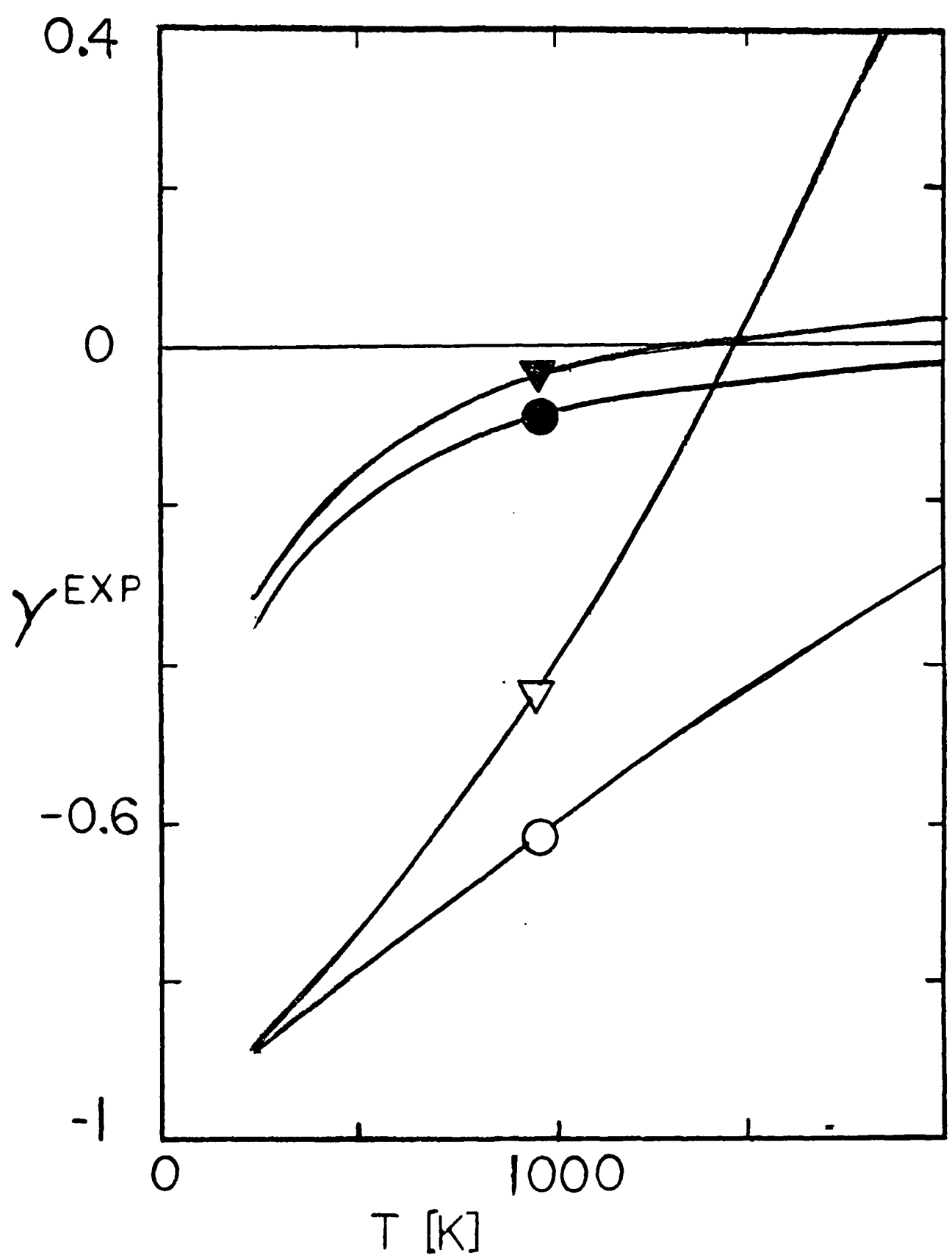
Fig 3: Plots of R_γ [$= |(\gamma^{\text{EXP}} - \gamma^{\text{EXP}}(\text{exact})) / \gamma^{\text{EXP}}(\text{exact})|$] vs E'_e ($=\langle\Delta E\rangle_d/RT_e^{\text{TR}}$) for CH_3NC (circles) and cycloheptatriene (triangles) with step sizes of 100 (broken line) and 1600 (solid line) cm^{-1} using TR, BG and T approximations for the EXP model. For all $R_\gamma < 0.001$ the data points are placed on the abscissa (see text). The filled symbols are for $R_\gamma > 0$ while the unfilled symbols are for $R_\gamma < 0$. The difference between filled and unfilled symbols with the same E'_e is larger than what appears on the plot. Nonetheless, the absolute errors (comparison with the exact calculations) are correctly represented.

Fig 4: Plots of $\gamma^{\text{EXP}}(\text{exact})$ vs temperature for methyl isocyanide (circles) and cycloheptatriene (triangles) with $\langle\Delta E\rangle_d$ of 100 (filled symbols) and 1600 (open symbols) cm^{-1} .



Handwritten signature or note





Enthalpy of formation

DISTRIBUTION LIST6/81
January 1985

	<u>No. Copies</u>		<u>No. Copies</u>
Dr. L. V. Schmidt Assistant Secretary of the Navy (R,E, and S) Room 5E 731 Pentagon Washington, DC 20350	1	Dr. L. H. Caveny Air Force Office of Scientific Research Directorate of Aerospace Sciences Bolling Air Force Base Washington, DC 20332	1
Dr. A. L. Slafkosky Scientific Advisor Commandant of the Marine Corps Code RD-1 Washington, DC 20380	1	Mr. Donald L. Ball Air Force Office of Scientific Research Directorate of Chemical Sciences Bolling Air Force Base Washington, DC 20332	1
Dr. Richard S. Miller Office of Naval Research Code 432 Arlington, VA 22217	10	Dr. John S. Wilkes, Jr. FJSRL/NC USAF Academy, CO 80840	1
Mr. David Siegel Office of Naval Research Code 260 Arlington, VA 22217	1	Dr. Philip Howe Army Ballistic Research Labs ARRADCOM Code DRDAR-BLT Aberdeen Proving Ground, MD 21005	1
Office of Naval Research Western Office 1030 East Green Street Pasadena, CA 91106		Mr. L. A. Watermeier Army Ballistic Research Labs ARRADCOM Code DRDAR-BLI Aberdeen Proving Ground, MD 21005	1
Dr. Larry Peebles Office of Naval Research East Central Regional Office 666 Summer Street, Bldg. 114-D Boston, MA 02210	1	Dr. W. W. Wharton Attn: DRSMI-RKL Commander U.S. Army Missile Command Redstone Arsenal, AL 35898	1
Dr. Phillip A. Miller Office of Naval Research Naval Station, Treasure Island Bldg. 7, Rm. 81 San Francisco, CA 94130	1	Mr. J. Murrin Naval Sea Systems Command Code 62R2 Washington, DC 20362	1
Mr. Otto K. Heiney AFATL - DLDL Eglin AFB, FL 32542	1	Dr. P. J. Pastine Naval Surface Weapons Center Code R04 White Oak Silver Spring, MD 20910	1
Mr. R. Geisler ATTN: MKP/MS24 AFRPL Edwards AFB, CA 93523	1	Mr. L. Roslund Naval Surface Weapons Center Code R122 White Oak Silver Spring, MD 20910	1
Dr. F. Roberto Code AFRPL MKPA Edwards AFB, CA 93523	1		

INIT

DISTRIBUTION LIST6/81
January 1985

	<u>No. Copies</u>		<u>No. Copies</u>
Mr. M. Stosz Naval Surface Weapons Center Code R121 White Oak Silver Spring, MD 20910	1	Dr. A. Faulstich Chief of Naval Technology MAT Code 0716 Washington, DC 20360	1
Dr. E. Zimmet Naval Surface Weapons Center Code R13 White Oak Silver Spring, MD 20910	1	LCDR J. Walker Chief of Naval Material Office of Naval Technology MAT, Code 0712 Washington, DC 20360	1
Dr. D.R. Derr Naval Weapons Center Code 388 China Lake, CA 93555	1	Dr. G. Bosmajian Applied Chemistry Division Naval Ship Reserve & Development Center Annapolis, MD 21401	1
Mr. Lee N. Gilbert Naval Weapons Center Code 3205 China Lake, CA 93555	1	Mr. R. Brown Naval Air Systems Command Code 330 Washington, DC 20361	1
Dr. E. Martin Naval Weapons Center Code 3858 China Lake, CA 93555	1	Dr. H. Rosenwasser Naval Air Systems Command AIR-310C Washington, DC 20360	1
Mr. R. McCarten Naval Weapons Center Code 3272 China Lake, CA 93555	1	Mr. B. Sobers Naval Air Systems Command Code 03P25 Washington, DC 20360	1
Dr. A. Nielsen Naval Weapons Center Code 385 China Lake, CA 93555	1	Dr. L. R. Rothstein Assistant Director Naval Explosives Dev. Engineering Dept. Naval Weapons Station Yorktown, VA 23691	1
Dr. R. Reed, Jr. Naval Weapons Center Code 388 China Lake, CA 93555	1	Dr. Lionel Dickinson Naval Explosive Ordnance Disposal Tech. Center Code D Indian Head, MD 20640	1
Dr. L. Smith Naval Weapons Center Code 3205 China Lake, CA 93555	1	Mr. C. L. Adams Naval Ordnance Station Code PM4 Indian Head, MD 20640	1
Dr. B. Douda Naval Weapons Support Center Code 5042 Crane, IN 47522	1	Mr. S. Mitchell Naval Ordnance Station Code 5253 Indian Head, MD 20640	1

DISTRIBUTION LIST6/81
January 1985

	<u>No. Copies</u>		<u>No. Copies</u>
Dr. William Tolles Dean of Research Naval Postgraduate School Monterey, CA 93940	1	Dr. R. G. Rhoades Commander Army Missile Command DRSMI-R Redstone Arsenal, AL 35898	1
Naval Research Lab. Code 6100 Washington, DC 20375	1	Dr. A. W. Barrows Ballistic Research Laboratory DRXBR-IBD Aberdeen Proving Ground, MD 21005	1
Dr. J. Schnur Naval Research Lab. Code 6510 Washington, DC 20375	1	Defense Technical Information Center DTIC-DDA-2 Cameron Station Alexandria, VA 22314	12
Mr. R. Beauregard Naval Sea Systems Command SEA 64E Washington, DC 20362	1	Dr. Ronald L. Simmons Hercules Inc. Eglin AFATL/DL DL Eglin AFB, FL 32542	1
Mr. G. Edwards Naval Sea Systems Command Code 62R3 Washington, DC 20362	1		
Mr. John Boyle Materials Branch Naval Ship Engineering Center Philadelphia, PA 19112	1		
Dr. H. G. Adolph Naval Surface Weapons Center Code R11 White Oak Silver Spring, MD 20910	1	Strategic Systems Project Office 1 Propulsion Unit Code SP2731 Department of the Navy Washington, DC 20376	
Dr. T. D. Austin Naval Surface Weapons Center Code R16 Indian Head, MD 20640	1	Mr. E.L. Throckmorton Strategic Systems Program Office Code SP-2731 Washington, DC 20376	1
Dr. T. Hall Code R-11 Naval Surface Weapons Center White Oak Laboratory Silver Spring, MD 20910	1	Dr. R. F. Walker USA ARRADCOM DRDAR-LCE Dover, NJ 07801	1
Mr. G. L. Mackenzie Naval Surface Weapons Center Code R101 Indian Head, MD 20640	1	Mr. J.M. Frankle Army Ballistic Research Labs ARRADCOM Code DRDAR-BLI Aberdeen Proving Ground, MD 21005	1
Dr. K. F. Mueller Naval Surface Weapons Center Code R11 White Oak Silver Spring, MD 20910	1	Dr. Ingo W. May Army Ballistic Research Lab AARADCOM Code DRDAR-BLI Aberdeen Proving Ground, MD 21005	1

DISTRIBUTION LIST6/81
January 1985

	<u>No. Copies</u>		<u>No. Copies</u>
E. J. Palm Commander Army Missile Command DRSMI-RK Redstone Arsenal, AL 35898	1	Dr. A. Karo Department of Chemistry & Materials Science L-325 Lawrence Livermore National Lab. Livermore, CA 94550	1
Dr. G. Neece Office of Naval Research Code 413 Arlington, VA 22207	1	Prof. Julius Mack 7030 Oregon Ave. N.W. Washington, DC 20015	1
Dr. L. D. Gardner Smithsonian Astrophysical Observatory 60 Garden Street Cambridge, MA 02138	1	Dr. S. Sheffield Sandia Laboratories Division 2513 P.O. Box 5800 Albuquerque, NM 87185	1
Dr. E. Grant Department of Chemistry Cornell University Ithaca, New York 14853	1	Prof. Curt Wittig University of Southern California Department of Chemistry Los Angeles, CA 90089-0484	1
Dr. K. Kirby Center for Astrophysics 60 Garden Street Cambridge, MA 02138	1	Dr. F. F. Crim Department of Chemistry University of Wisconsin Madison, Wisconsin 53706	1
Dr. W. A. Lester, Jr. Department of Chemistry University of California Berkeley, CA 94720	1	Dr. Peter Bernath University of Arizona Department of Chemistry Tucson, AZ 85721	1
Prof. Richard A. Reinhardt Naval Postgraduate School Physics & Chemistry Dept. Monterey, CA 93940	1	Dr. M. Cowperthwaite SRI International 333 Ravenswood Avenue Menlow Park, CA 94025	1
Dr. T. Rivera Los Alamos National Lab. Explosives Technology MS C920 Los Alamos, New Mexico 87145	1	Dr. G. Adams DRXBR-IBD Ballistics Research Laboratory Aberdeen Proving Ground, MD 21005	1
Dr. Andrew C. Victor Naval Weapons Center Code 3208 China Lake, CA 93555	1	Dr. R. B. Kruse Morton Thiokol, Inc. Huntsville Division Huntsville, AL 35807-7501	1
Dr. D. M. Golden SRI International 333 Ravenswood Avenue Menlo Park, CA 94025	1	Dr. R. E. Wyatt Department of Chemistry University of Texas Austin, TX 78712	1
Dr. M. E. Jacox Molecular Spectroscopy Div. National Bureau of Standards Gaithersburg, MD 20899	1	Prof. John H. Clark Department of Chemistry University of California Berkeley, California 94720	1

INIT

DISTRIBUTION LIST6/81
January 1985

	<u>No. Copies</u>		<u>No. Copies</u>
Dr. Tim Parr Naval Weapons Center Code 3891 China Lake, CA 93555	1	Dr. B. Swanson INC-4 MS C-346 Los Alamos National Laboratory Los Alamos, NM 87545	1
Dr. R. R. Alfano Institute for Ultrafast Spectroscopy and Lasers-CCNY-Physics 138th Street Convent New York, New York 10031	1	Dr. Rodney J. Bartlett Quantum theory Project Williamson Hall University of Florida Gainesville, FL 32611	1
Dr. Steve Agnew INC-4, MS C346 Los Alamos National Laboratory Los Alamos, New Mexico 82545	1	Dr. B. Junker Office of Naval Research Code 412 800 N. Quinicy Street Arlington, VA 22217	1
Dr. Stephen L. Rodgers AFRPL/LKLR Edwards AFB, CA 93523	1	Prof. H. A. Rabitz Department of Chemistry Princeton University Princeton, NH 08540	1
Dr. T. L. Boggs Naval Weapons Center Code 3891 China Lake, CA 93555	1	Dr. M. Farber Space Sciences, Inc. 135 West Maple Avenue Monrovia, CA 91016	1
D. Curran SRI International 333 Ravenswood Avenue Menlo Park, CA 94025	1	Professor G. D. Duvall Washington State University Department of Physics Pullman, WA 99163	1
Prof. Kenneth Kuo Pennsylvania State University Dept. of Mechanical Engineering University Park, PA 16802	1	Professor Y. T. Lee Department of Chemistry University of California Berkeley, CA 94720	1
Dr. James T. Bryant Naval Weapons Center Code 3205B China Lake, CA 93555	1	Dr. R. Bernecker Code R13 Naval Surface Weapons Center White Oak Silver Spring, MD 20910	1
Dr. W. L. Faust Naval Research Laboratory Code 6510 Washington, DC 20375	1	Dr. C. S. Coffey Naval Surface Weapons Center Code R13 White Oak Silver Spring, MD 20910	1
Dr. J.M. Culver Strategic Systems Projects Office SSPD/SP-2731 Crystal Mall #3, RM 1048 Washington, DC 20376	1	Dr. P. Rentzepis Bell Laboratories Murray Hill, NJ 07971	1
Dr. Y. M. Gupta Shock Dynamics Laboratory Department of Physics Washington State University Pullman, WA 99164	1		

END

FILMED

1-86

DTIC